POINT CLOUD TRANSFORMATION USING SENSOR CALIBRATION INFORMATION FOR MAP DATA ADJUSTMENT

J. Lee [1], J. Bae [1], Y. Choi [1], I. Park [1], S. Hong [2], H. Sohn [1] *

[1]Yonsei University, Civil & Environmental Engineering Ph.D candidate, Yonsei-ro 50 Seoul, Korea - (ontheground, junsu510, qwas6456, yoonjo15)@yonsei.ac.kr
[1*]Yonsei University, Civil & Environmental Engineering Faculty, Yonsei-ro 50 Seoul, Korea – sohn1@yonsei.ac.kr
[2] Stryx. co, CTO, Yonsei-ro 50-1 Seoul, Korea, - cto@stryx.co.kr

KEY WORDS: Point cloud, Mobile mapping system, Calibration, High-precision map, LiDAR, Bird eye's view

ABSTRACT:

In order to operate autonomous vehicles and unmanned delivery vehicle, it is important to accurately acquire location of the device itself. However, since these devices are mainly operated in urban areas, there is a limit in obtaining location information based on GNSS. Therefore, it is necessary to utilize a method of calibrating its own location information by measuring the reference point provided by the existing high-precision map of the region. Point cloud based multi-dimensional high-precision maps are acquired in advance using high-performance LiDAR and GNSS devices for infrastructure such as roads, and provide a reference point for autonomous driving or map updating. Since such high-performance surveying equipment requires high cost, it is difficult to attach to autonomous vehicles or unmanned vehicle for commercialization. Therefore, autonomous vehicles or unmanned delivery vehicle are operated with relatively low performance LiDAR and GNSS, so it is often impossible to accurately measure the reference point, which directly leads to a decrease in the accuracy of the location information of the device. To compensate for this, this study proposes a point interpolation method to extract GCP information from sparse point cloud maps acquired with low performance LiDAR. The proposed method uses calibration parameters between point data and the image data acquired from the device. In general, images provide higher resolution than point clouds, even when using low-end cameras, so that the position of point coordinates relative to a reference point can be measured relatively accurately from the image and projection data of the point cloud. The data acquisition vehicle is an MMS vehicle that provides a panoramic image using four DSLRs and a point cloud with Velodyne VLP 16. The researchers first conducted a reference point survey on features such as road signs. The panorama image including the road sign was transformed into a bird eye's view, and point projection was performed on the bird eye's view image. The reference point coordinates, which were not acquired by the point cloud, were obtained from the shape of the road sign in the bird eye's view image, and the accuracy was compared with the measured data.

1. INTRODUCTIONS

Construction of multi-channel spatial information has become an essential element in the construction of smart cities (Gruen, 2013; Roche, 2014). This is because it is essential to build accurate spatial information to implement infrastructure management, which is a core element of smart cities, and to operate unmanned moving objects (Um, 2017; Xie et al., 2019). However, urban spatial information such as roads has the characteristic of changing from moment to moment. Because dynamic city changes cannot be controlled, mapping update vehicles must be continuously operated in the city to keep the latest spatial information at all times. This mapping update vehicle measures and reflects the changes in the city from time to time in reference data that are very precisely constructed with ground LiDARs. Therefore, a number of mapping update vehicles are operated at all times, so it is necessary to detect changes in the city (Anjomshoaa et al., 2018).
The mapping update vehicle is equipped with a LiDAR for point cloud, image sensor, and GNSS / INS equipment. The core data is a point cloud that acquires spatial information, which has a very low point density than the initial reference data due to the characteristics of a mobile-operated mapping update vehicle.

Occasional occlusion of GNSS data occurs in urban areas. Especially, the occlusion of GNSS data is very large in the sections such as under the bridge and overpass, so the mapping update accuracy of the vehicle updating the map based on the GNSS location falls (Groves et al., 2012; Wang et al., 2013; Zhu et al., 2018). Therefore, in preparation for such a case, the mapping update vehicle measures the same point as the previously measured reference point on the reference data during operation, and corrects location information through comparison between the measured value and the reference value. These reference points are constructed in the form of points, and the correction amount is also accurate when very precise surveying is done in points. However, due to the nature of the mobile mapping system that acquires data at the same time as running, due to the lack of equipment point density and rapid movement, accurate point-by-point measurement of the reference point location is often not performed. Therefore, if point-by-point measurement of the reference point is not possible, a process of supplementing the reference point through interpolation from the surrounding coordinate system is necessary. Through the acquisition of the reference point through interpolation, it is expected that the accuracy of the map constructed by the mapping update vehicle will be improved.

* Corresponding author

2. MATERIALS

2.1 Data acquisition

Data acquisition is performed along bicycle roads in Seoul, Korea using our own MMS (Hong et al., 2017). Among the acquired MMS point clouds, data of areas where the GNSS accuracy of the point cloud decreases while passing under the bridge was extracted. As shown below, 44 points of GNSS was surveyed by selecting an area where GNSS is unstable due to occlusion under the pier, etc., and compared with coordinates obtained by MMS.

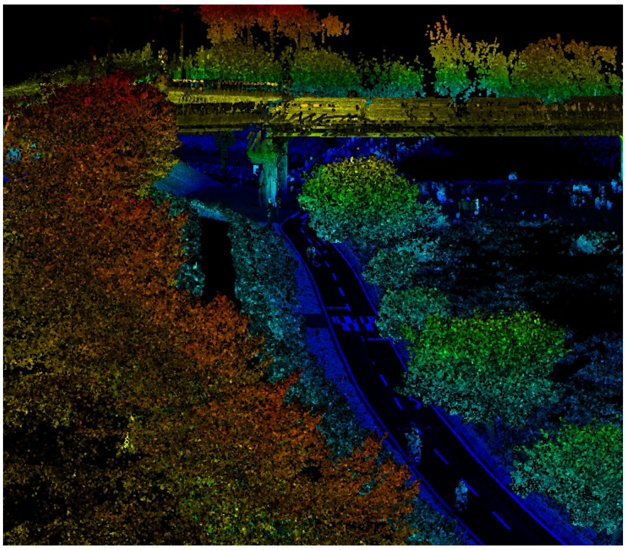

Figure 1. Pointcloud of test site (colors represent height)

2.2 Methods

In this study, calibration information between MMS devices and previously acquired reference point coordinates were used as a supplementary method for reference point surveying for map update vehicles. The MMS system acquires various data such as images, GNSS, and point clouds from various sensors on board, and these c can be fused by MMS bore-sight and lever-arm calibration.

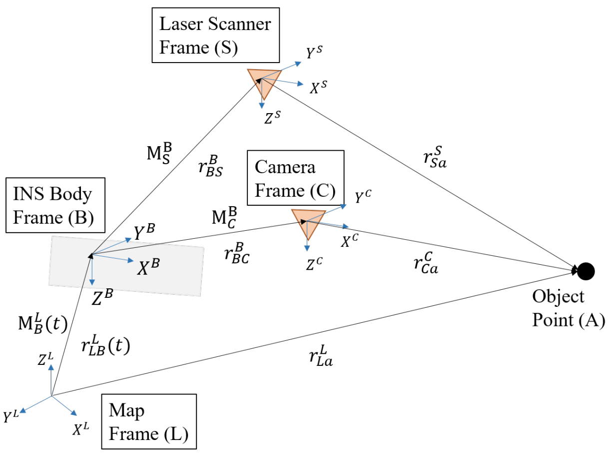

Figure 2. Geometric relation among MMS sensors

As shown in the figure, the coordinate relationship among the object point(A), LiDAR frame(S), camera frame(C), INS body frame(B) and map frame(L) can be expressed mathematically through rotation and translation among coordinate systems. The coordinate system of the image and the LiDAR is integrated based on the INS coordinate system, which is then projected onto the map coordinate system. The mathematical model expressing the geometric relationship can be defined by Equation (1).

$$r_{La}^{L} = r_{LS}^{L}(t) + M_{B}^{L}(t)(M_{S}^{B} r_{Sa}^{S} + r_{BS}^{B}) \qquad (1)$$

where r_{La}^{L} = coordinate of map frame
t = observation time
$r_{La}^{L}(t)$ = position of the INS body frame in the map frame
$M_{B}^{L}(t)$ = rotation matrix from the INS body frame to the map frame
M_{S}^{B} = rotation matrix from the LiDAR frame to the INS body frame
r_{BS}^{B} = position of the LiDAR in the INS body frame

The MMS system acquires various data such as images, GNSS, and point clouds from various sensors on board, and these data can be fused by MMS bore-sight and lever-arm calibration. And all the sensors in the MMS were time-synchronized, so that they were configured to acquire data almost simultaneously with the moving MMS. These simultanesou data acquisitions occurr within a short frequency period of 10Hz, and formed a s et to record the spatial data concretely. A set of data from the GNSS/INS, camera image, and LiDAR point cloud acquired at the same moment can be integrated within the same frame. The point cloud is linked to GNSS data and measured in absolute coordinates, which are projected onto image pixels. Therefore, if the absolute coordinate value of an arbitrary position value acquired in the image is known, on the contrary, it is possible to interpolate the error of the point cloud through comparison with the coordinate value of the point cloud acquired by the LiDAR of the device. Therefore, even if the mounted LiDAR does not accurately measure the reference point and thus does not acquire the reference point, if it is acquired as a high-resolution image, it can be estimated by interpolating point coordinates from the location of the previously acquired reference point shown in the image. Each individually acquired data value is integrated and expressed as shown in Figure 3. By projecting the point cloud with absolute coordinates onto the images, the absolute coordinates of the desired objects can be obtained.

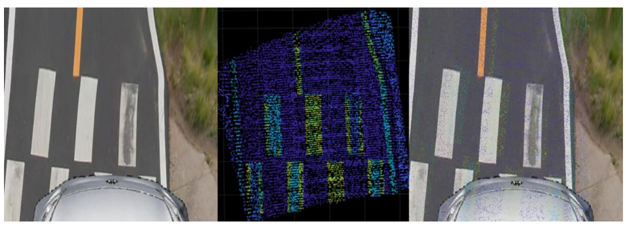

Figure 3. Example of acquired data, image (left)/ point cloud (middle)/ projection of both data (right), (colors represent point intensity)

The workflow is shown in Figure 4 below. The LiDAR and the camera attached to the MMS move along the road and proceed with the mapping. In the meantime, coordinate of a target point whose coordinate is already acquired by precise GNSS device, is also acquired. The error between the coordinates acquired by the LiDAR and the previously acquired GNSS reference is confirmed through the visual error check through point projection between image and point cloud.

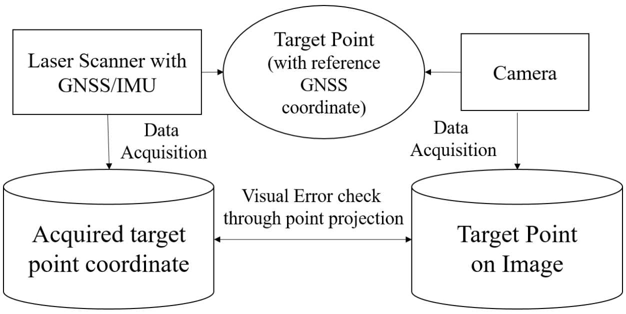

Figure 4. Schematic workflow

As shown in Figure 5, the location of the previously acquired reference point (yellow dot) appears in the image, and similarly, the reference point (red dot) acquired by MMS can also be displayed on the image through projection by the MMS geometric relationship. And acquisition errors can be visually checked since both points of GNSS reference and MMS LiDAR acquired are coupled through the point projection.

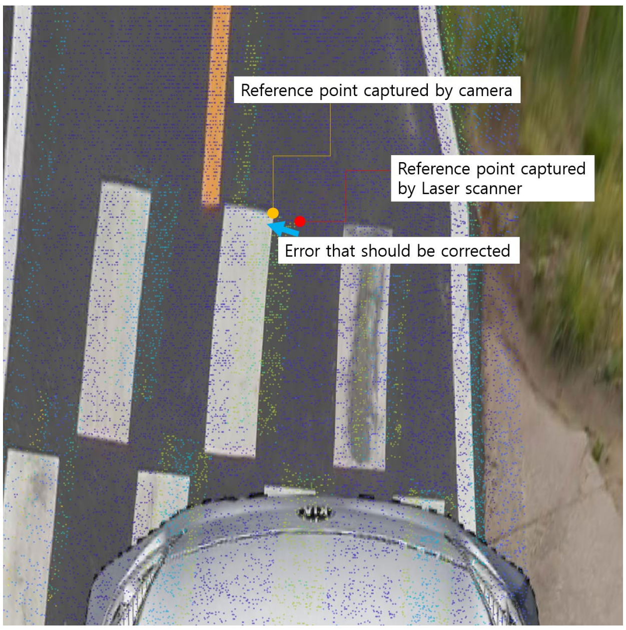

Figure 5. Error in obtaining MMS location information through the reference point shown in the image

After assuming that the coordinate value of the reference point acquired by the LiDAR contains an error, the conversion coefficient between the reference point data was calculated through LESS analysis with the value previously acquired by the precise GNSS device, and then applied to the correction of the remaining mapping point values. The transformation is assumed as 3D transformation on homogeneous coordinate system.
33 out of 44 target points were used as GCP and the remaining 11 points (point number 5, 9, 13, 17, 21,25, 29, 33, 37, 41) were used as check points to understand the effect of improving data accuracy.

3. RESULT

Before data coupling and coordinate adjustment through image projection, the measurement error of MMS for 33 reference points was 0.0967m, but after correction of point cloud coordinates through coordinate adjustment, the error amount for 11 checkpoints was improved to 0.053m.
The data used are shown as tables below. Table 1 and Table 2 below show the coordinates of GCPs obtained by GNSS and MMS respectively.

Point number	GNSS acquired coordinate of Ground Control Points (m)		
	X	Y	Z
1	189538.666	546483.033	31.18392
2	189539.781	546481.043	31.1891
3	189541.37	546484.828	31.08618
4	189537.498	546484.603	31.19185
6	189539.433	546476.978	31.2412
7	189540.252	546475.139	31.29146
8	189538.922	546473.044	31.28275
10	189540.546	546469.086	31.33291
11	189538.866	546468.187	31.31806
12	189539.502	546465.818	31.33996
14	189542.119	546463.909	31.37323
15	189541.672	546462.311	31.35484
16	189539.64	546464.474	31.33923
18	189540.556	546460.087	31.33504
19	189539.863	546454.005	31.27491
20	189540.92	546453.965	31.28363
22	189538.803	546405.756	31.15608
23	189534.573	546385.931	31.15789
24	189535.452	546385.792	31.1868
26	189536.803	546382.891	31.21148
27	189536.409	546380.503	31.2091
28	189535.53	546380.651	31.18061
30	189533.301	546380.998	31.16604
31	189536.096	546376.993	31.25598
32	189534.329	546377.286	31.19714
34	189531.805	546358.658	31.20237
35	189532.056	546357.075	31.22924
36	189531.031	546357.179	31.2191
38	189529.24	546347.303	31.23134
39	189530.17	546348.207	31.2591
40	189529.835	546345.186	31.27405
42	189528.779	546346.03	31.27783
43	189529.116	546345.001	31.26711

Table 1. Previously acquired coordinates of Ground Control Points acquired by GNSS device

Point number	MMS acquired coordinate of Ground Control Points (m)		
	X	Y	Z
1	189538.599	546483.041	31.26
2	189539.732	546481.051	31.27
3	189541.321	546484.781	31.16
4	189537.443	546484.671	31.3
6	189539.387	546477.06	31.35
7	189540.221	546475.198	31.34
8	189538.882	546473.111	31.37
10	189540.525	546469.16	31.4
11	189538.81	546468.221	31.41
12	189539.462	546465.87	31.39
14	189542.095	546463.9	31.42
15	189541.656	546462.294	31.42
16	189539.594	546464.474	31.4
18	189540.524	546460.101	31.39
19	189539.832	546454.021	31.34
20	189540.909	546453.98	31.34
22	189538.773	546405.791	31.18
23	189534.555	546386.021	31.19
24	189535.881	546385.681	31.19
26	189536.793	546382.952	31.23
27	189536.407	546380.521	31.25
28	189535.547	546380.682	31.22
30	189533.291	546381.031	31.2
31	189536.09	546377	31.26
32	189534.332	546377.371	31.23
34	189531.845	546358.681	31.3
35	189532.096	546357.071	31.3
36	189531.053	546357.293	31.31
38	189529.255	546347.401	31.34
39	189530.203	546348.242	31.33
40	189529.861	546345.169	31.34
42	189528.793	546346.051	31.34
43	189529.152	546345.05	31.35

Table 2. Coordinates of Ground Control Points acquired by MMS device

Table 3 below shows the coordinates of 10 checkpoints obtained by GNSS.

Point number	GNSS acquired Coordinate of check points (m)		
	X	Y	Z
5	189541.785	546478.619	31.26357
9	189539.636	546471.66	31.29815
13	189541.591	546465.35	31.37392
17	189539.079	546462.918	31.33957
21	189537.754	546405.877	31.12744
25	189536.774	546385.568	31.20215
29	189534.634	546380.796	31.16963
33	189534.086	546375.837	31.20782
37	189528.899	546349.354	31.24016
41	189528.625	546346.874	31.24895

Table 3. Check point coordinates acquired by GNSS device

Table 4 below shows the coordinates of 10 checkpoints obtained by MMS.

Point number	MMS acquired Coordinate of check points (before transformation) (m)		
	X	Y	Z
5	189541.774	546478.65	31.33
9	189539.592	546471.701	31.37
13	189541.57	546465.333	31.42
17	189539.034	546462.982	31.41
21	189537.722	546405.95	31.18
25	189536.772	546385.532	31.21
29	189534.632	546380.83	31.21
33	189534.104	546375.941	31.23
37	189528.942	546349.459	31.33
41	189528.644	546346.92	31.33

Table 4. Check point coordinates acquired by MMS (before adjustment)

Table 5 below show the adjusted result of checkpoints by LESS analysis. After LESS adjustment, the checkpoint values obtained by MMS become closer to the coordinate values of checkpoints obtained by GNSS.

Point number	MMS acquired Coordinate (before transformation) (m)		
	X	Y	Z
5	189541.813	546478.623	31.26
9	189539.637	546471.669	31.294
13	189541.613	546465.295	31.338
17	189539.08	546462.945	31.329
21	189537.691	546405.932	31.14
25	189536.732	546385.508	31.167
29	189534.593	546380.806	31.167
33	189534.066	546375.915	31.184
37	189528.911	546349.421	31.27
41	189528.611	546346.882	31.27

Table 5. Check point coordinates adjusted

4. CONCLUSION

It is very important to accurately understand the current location of the device in order to ensure the safe operation of autonomous vehicles and the high positioning accuracy of mapping vehicles such as MMS that creat a high definition base map. However, it is difficult to obtain accurate location information of a device when passing a GNSS occluded area, such as under a bridge, beside a building.

In this study, sensor calibration information was used to reduce the data error, when operating an MMS that acquires data simultaneously with the operation. The proposed method uses calibration parameters between point data and the image data acquired from the device. In general, images provide higher resolution than point clouds, even when using low-end cameras, so that the position of point coordinates relative to a reference point can be measured relatively accurately from the image and projection data of the point cloud. The point cloud coordinate error that occurs when acquiring data with MMS was corrected through applying the transformation information between the couple of reference point coordinates acquired by a high-precision GNSS and MMS-equipped LiDAR.

The couple matching of two coordinate data was performed through projection of image and point cloud using the sensor calibration information as bore-sight and lever-arm calibration. As a result, the data acquisition error of 0.0967 m before correction could be reduced to 0.053 m.

https://doi.org/10.5194/isprs-archives-XLIII-B3-2020-521-2020 | © Authors 2020. CC BY 4.0 License.

However, the proposed method has limitations that the reference coordinates of Ground Control Points should be previously acquired and properly managed so that the method can utilize the information.
If automation of reference point detection is achieved through further research such as image matching, it is expected to contribute to automatic map update using MMS.

ACKNOWLEDGEMENTS

This research was supported by a grant from the Water Management Research Program funded by Ministry of Land, Infrastructure and Transport of Korean government (20AWMP-B121100-05).

And we would like to thank Editage (www.editage.co.kr) for English language editing.

REFERENCES

Anjomshoaa, A., Duarte, F., Rennings, D., Matarazzo, T.J., Desouza, P., Ratti, C., 2018. City Scanner: Building and Scheduling a Mobile Sensing Platform for Smart City Services. IEEE Internet Things J. 5, 4567–4579. https://doi.org/10.1109/JIOT.2018.2839058

Groves, P.D., Jiang, Z., Wang, L., Ziebart, M.K., 2012. Intelligent Urban Positioning using Multi- Constellation GNSS with 3D Mapping and NLOS Signal Detection. 25th Int. Tech. Meet. Satell. Div. Inst. Navig. TN.

Gruen, A., 2013. SMART cities: The need for spatial intelligence. Geo-Spatial Inf. Sci. 16, 3–6. https://doi.org/10.1080/10095020.2013.772802

Hong, S., Park, I., Lee, J., Lim, K., Choi, Y., Sohn, H., 2017. Utilization of a Terrestrial Laser Scanner for the Calibration of Mobile Mapping Systems. Sensors 17(3), 474. https://doi.org/10.3390/s17030474

Roche, S., 2014. Geographic Information Science I: Why does a smart city need to be spatially enabled? Prog. Hum. Geogr. 38, 703–711. https://doi.org/10.1177/0309132513517365

Um, J.-S., 2017. Embracing cyber-physical system as cross-platform to enhance fusion-application value of spatial information. Spat. Inf. Res. 25, 439–447. https://doi.org/10.1007/s41324-017-0112-8

Wang, L., Groves, P.D., Ziebart, M.K., 2013. GNSS shadow matching: Improving urban positioning accuracy using a 3D city model with optimized visibility scoring scheme. Navig. J. Inst. Navig. 60, 195–207. https://doi.org/10.1002/navi.38

Xie, Y., Gupta, J., Li, Y., Shekhar, S., 2019. Transforming Smart Cities with Spatial Computing. 2018 IEEE Int. Smart Cities Conf. ISC2 2018 1–9. https://doi.org/10.1109/ISC2.2018.8656800

Zhu, N., Marais, J., Betaille, D., Berbineau, M., 2018. GNSS Position Integrity in Urban Environments: A Review of Literature. IEEE Trans. Intell. Transp. Syst. 19, 2762–2778. https://doi.org/10.1109/TITS.2017.2766768